METRICA
METRology Institutional CAtalog

ISTITUTO NAZIONALE DI RICERCA METROLOGICA
Repository Istituzionale

The Earth's magnetic field in Italy during the Neolithic period: New data from the Early Neolithic site of Portonovo (Marche, Italy)

This is the author's submitted version of the contribution published as:

Original
The Earth's magnetic field in Italy during the Neolithic period: New data from the Early Neolithic site of Portonovo (Marche, Italy) / Tema, Evdokia; Ferrara, Enzo; Camps, Pierre; Conati Barbaro, Cecilia; Spatafora, Simone; Carvallo, Claire; Poidras, Thierry. - In: EARTH AND PLANETARY SCIENCE LETTERS. - ISSN 0012-821X. - 448:(2016), pp. 49-61. [10.1016/j.epsl.2016.05.003]

Availability:
This version is available at: 11696/54727 since: 2017-02-28T17:16:42Z

Publisher:
Elsevier

Published
DOI:10.1016/j.epsl.2016.05.003

Terms of use:

This article is made available under terms and conditions as specified in the corresponding bibliographic description in the repository

Publisher copyright

(Article begins on next page)

25 April 2024

The Earth's magnetic field in Italy during the Neolithic period: New data from the Early Neolithic site of Portonovo (Marche, Italy)

Evdokia Tema[a,b,*], Enzo Ferrara[c], Pierre Camps[d], Cecilia Conati Barbaro[e], Simone Spatafora[c], Claire Carvallo[f], Thierry Poidras[d]

[a]*Dipartimento di Scienze della Terra, Università degli Studi di Torino, via Valperga 35, 10125, Torino, Italy, evdokia.tema@unito.it*

[b]*ALP-Alpine Laboratory of Palaeomagnetism, via G.U. Luigi Massa 6, 12016, Peveragno, Italy*

[c]*Istituto Nazionale di Ricerca Metrologica, Strada delle Cacce 91, I-10135 Torino, Italy, e.ferrara@inrim.it, simone.spatafora@edu.unito.it*

[d]*Géosciences Montpellier, CNRS and Université Montpellier, Montpellier, France, pierre.camps@umontpellier.fr, poidras@gm.univ-montp2.fr*

[e]*Dipartimento di Scienze dell'Antichità, Sapienza Università di Roma, Roma, Italy, cecilia.conati@uniroma1.it*

[f]*Institut de Minéralogie, de Physique des Matériaux et de Cosmochimie (IMPMC), Sorbonne Universités, Paris, France, Claire.Carvallo@impmc.upmc.fr*

** Corresponding author: Tel. +39 011 6708395, Fax. +39 011 6708398*

ABSTRACT

We present new, full geomagnetic field vector results from three Neolithic ovens discovered at the archaeological site of Portonovo (Marche, Italy). The discovered structures are a rare example of very well preserved underground ovens from the Early Neolithic period. Standard thermal demagnetization procedures were used to isolate the direction of the Characteristic Remanent Magnetization acquired by the baked clay during the ovens' last firing. The corresponding archaeointensities

were determined by the multi-specimen procedure (MSP-DSC) and show a clear intensity low during the Neolithic period. Both directional and intensity results are of high quality, offering the first contribution of full geomagnetic field vector data for this period in Italy. The new data are compared with other contemporaneous data from Europe and with global geomagnetic field models. Independent archaeomagnetic dating of the three ovens was also performed by means of the SCHA.DIF.14k model. The obtained results are in excellent agreement with available radiocarbon dates and confirm that all ovens belong to the Neolithic. These new data importantly enrich our knowledge of the geomagnetic field during the Neolithic period that is poorly documented by data, not only in Italy but also in the whole of Europe and show that archaeomagnetic dating can provide precise results even for prehistoric periods.

Keywords: Palaeosecular variation; archaeomagnetism; oven; Neolithic; Italy

1. Introduction

Archaeomagnetic data from ancient baked clay archaeological structures is a precious source of information about the past variations of the Earth's magnetic field. Thanks to archaeomagnetic records from well dated archaeological artefacts, it is possible to model the variations of the geomagnetic field in the past and better understand its past behaviour. Up to now, local Secular Variation (SV) curves have been established for several countries, mainly in Europe, and different geomagnetic field models have been proposed based on the available archaeomagnetic data at regional and global level. However, most of the proposed SV curves cover only the last three millennia, while the geomagnetic field variations in earlier times are still poorly described.

In Italy, Tema et al. (2006) have published a preliminary SV curve based on 65 directional results ranging in time from 1300 BC to 1700AD. More recently, Tema (2011) compiled an updated dataset of Italian archaeomagnetic data, presenting 73 directional and 23 intensity determinations. From these data, only six directional results come from material older than 1000 BC. This significant lack of data from periods previous to the first millennium BC can be attributed to several factors, including the very limited number of well preserved still *in situ* baked clay structures (often due to the use of poor building materials in prehistoric times) and the difficulty of precise independent dating of such old and badly preserved structures.

In this study, we present new, full geomagnetic field archaeomagnetic results from three Neolithic ovens excavated at the archaeological site of Portonovo (Marche, Italy). The discovered ovens are a rare example of very well preserved underground ovens and have the advantage of being from a well dated archaeological context with three radiocarbon dates. The new results are the first full geomagnetic field vector data available for this period in Italy and importantly enrich our knowledge about the geomagnetic field during the Neolithic period.

2. Archaeological site and sampling

The archaeological site of Portonovo Fosso Fontanaccia (43.56º N, 13. 57 °E), is situated on the Conero promontory, along the Adriatic coast of Marche (Ancona, Italy). It is located on a south-facing slope, along the right bank of the river Fontanaccia. It was first identified in the 1990s; since then, several excavation campaigns brought into light a total of 22 underground ovens, at different heights along the hillside (Fig. 1). The ovens were built by digging small cavities into the colluvial layer. Almost all of them overlook large depressions in front of their

78 openings. Six of the ovens were found totally intact (Conati Barbaro, 2013). Despite
79 their different states of preservation, all ovens share similar features and dimensions:
80 the base is circular, flat, with a slight central depression, made of yellow-reddish
81 smoothed clay lining, and measuring from 1.8 to 2.0 meters in diameter; the vaults are
82 very low, so that the maximum height in the six ovens found intact does not exceed
83 50 cm; the mouths are between 60 and 80 cm in width. The inner surfaces were
84 partially coated with clay and subsequently consolidated by the firing.

85 Information about the maximum firing temperatures reached during the use of
86 the Portonovo ovens was provided by X-ray powder diffraction analysis (PXRD),
87 based on the transformation of CaO-rich sediments, structurally modified by exposure
88 to low or high temperatures clay (Muntoni and Ruggiero, 2013). PXRD analysis
89 performed on 12 samples from the hardened baked clay of the ovens inner walls
90 revealed the predominance of calcite, a variable amount of quartz and a small
91 quantity of feldspars in all samples. It also revealed the absence of Ca-silicates newly
92 formed by exposure to high temperatures, such as diopsidic pyroxenes or gehlenite,
93 typical of CaO-rich clay (Muntoni and Ruggiero, 2013). These results suggest that the
94 sediments were heated at temperatures not higher than 500 °C (Muntoni and
95 Ruggiero, 2013). Based on these relative low heating conditions, the use of the ovens
96 for pottery production may be excluded, as in that case higher heating temperatures
97 would be expected. The presence of charred cereal grains, mainly barley, within
98 ovens 14, 15 and 16, leads to the hypothesis that they were used for food processing
99 and cooking, as well as for other purposes, such as heating flint. In fact, many blades
100 and bladelets found inside and outside the ovens show clear signs of thermal
101 treatment (Conati Barbaro, 2013). Moreover, two ovens contained three adult burials
102 (two in oven 1 and one in oven 5). The secondary use of domestic structures as

103 burials, which is quite a common funerary practice during the Neolithic, probably
104 occurred when the structure itself, or perhaps the entire area, lost their primary
105 function.

106 According to the archaeological evidence, the ovens were used in the same
107 time period but most likely not all of them at the same moment. Each oven was
108 probably constructed, used for few years and then abandoned, as there is no evidence
109 of maintenance to extend its functional life. After abandonment of one oven, another
110 one was made just next to the damaged one. Based on the decoration style of some
111 pottery found, the site could be linked to the middle-Adriatic *facies* of the Italian
112 ancient Neolithic (Conati Barbaro, 2013). The homogeneity of the materials and the
113 stratigraphic data also indicate that the site was occupied for a short period of time.
114 Dating obtained from radiocarbon analysis also supports this hypothesis. Three
115 radiocarbon dates have been obtained so far (Conati Barbaro, 2013), all of them
116 carried out at CEDAD (Centro di Datazione e Diagnostica) of the University of
117 Salento, Italy, using the Accelerator Mass Spectrometry (AMS) technique.
118 Radiocarbon results were calibrated using the OxCal 3.1 software after comparison
119 with the atmospheric data reference curves (Reimer at al., 2004; 2009) and calibrated
120 ages were calculated at 95% of probability. The oldest date, carried out on a barley
121 caryopsis found inside the oven 14, suggests a calibrated age 5620-5460 BC
122 (uncalibrated age 6555 ± 45 BP, Lab code: LTL12777A). The other two dates come
123 from findings inside the oven 5; one from charcoal collected from the floor of the
124 oven dated at 5560-5350 BC (uncalibrated age 6500 ± 50 BP, Lab code: LTL5192A),
125 and the other from a bone of the male burial dated at 5480-5310 BC (uncalibrated age
126 6418 ± 50 BP, Lab code: LTL5191A). Even though it is not possible to precisely date

the time of use and abandonment of each oven, it is however certain that all of them belong to the Early Neolithic period and they have been used between 5620-5310 BC.

For the archaeomagnetic study presented here, baked clay samples from the ovens 14 (PFO-14), 16 (PFO-16) and 17 (PFO-17) have been collected (Fig. 1). These ovens were excavated in 2013 and archaeomagnetic sampling was carried out in October 2013. All of the studied ovens were found intact, with their walls and vaults almost entirely preserved. Ovens PFO-14 and PFO-16 overlooked a large shallow pit. Unlike these, oven PFO-17 has a trapezoidal shape and was originally excavated on the edge of another pit. Ovens PFO-14 and PFO-16 were filled with organic sediment containing dozens of charred cereal grains. Archaeological findings, such as pottery and lithic artifacts, were rare within all the studied structures.

Initially, archaeomagnetic sampling was attempted with a portable rock drill. However, even though the baked clay that constituted the floor and the walls of the ovens was apparently compact, it proved to be extremely friable when drilled. Most of the drilled cores broke in small pieces when extracting them from the oven and thus they were only used for magnetic mineralogy analysis and archaeointensity determinations. Systematic sampling was therefore performed with non-magnetic cylindrical plastic boxes of standard dimensions (diameter= 25 mm, height= 20 mm). A total of 38 samples were collected from the floor of the three ovens (15 samples from oven PFO-14, 11 from oven PFO-16 and 12 from oven PFO-17). All of them were independently oriented *in situ* with a magnetic compass and an inclinometer.

3. Rock magnetic experiments

Detailed magnetic mineralogy experiments on representative samples from the three ovens have been performed in order to better understand the nature, the type, the

size and the thermal stability of magnetic minerals included in the collected baked clays.

3.1 Viscosity index

In order to investigate the stability of the magnetization carried by the studied samples, the viscosity index v (%) (Thellier and Thellier, 1944; Prévot, 1981) has been calculated for the whole sample collection. The remanent magnetization was first measured after a 15-days storage of the samples with their positive cylindrical axis oriented parallel to the laboratory ambient field. Next, the remanent magnetization was measured again after subsequent 15 days storage in zero field (shielded chamber). The viscosity index was then calculated as the vector difference between the two measurements. It was used as a quantitative estimate of the ratio of the Viscous Remanent Magnetization (VRM) acquired *in situ* until the sampling, to the primary remanent magnetization acquired during the last use of the ovens. For the majority of the samples, the viscosity index varies from 5% to 15 % and only for four samples from PFO-14 oven it is as high as 20 % (Fig. 2a). In order to guarantee that a possible VRM does not importantly affect our results, we have further stored all samples in zero field for 30 days before beginning the measurements.

3.2 Isothermal remanent magnetization curves

Isothermal remanent magnetization (IRM) curves have been obtained for nine samples (three from each oven) at the ALP Palaeomagnetic laboratory (Peveragno, Italy). An ASC pulse magnetizer was used to impart the IRM, applying stepwise increasing magnetic fields up to 1.6 T, and the remanent magnetization was measured with a JR6 spinner magnetometer (AGICO). The normalized IRM acquisition curves

obtained from the different samples are very similar and show that in most cases saturation is reached at applied fields of 0.2-0.4 T (Fig. 2b). These results suggest the presence of a low coercivity mineral as the main carrier of magnetization, most probably magnetite.

3.3 Thermal demagnetization of a three-axes IRM

An IRM was imparted with an ASC pulse magnetizer along three orthogonal axes of representative samples, applying first a maximum 1.6 T, then a medium 0.5 T and finally a minimum 0.1 T magnetic field. Stepwise thermal demagnetization of this composite IRM was performed to obtain unblocking temperatures of hard-, medium- and soft-magnetic components (Lowrie, 1990). The demagnetization curves obtained show that in all samples, most of the magnetization is carried by the magnetically soft fraction (< 0.1 T) while the medium and high-coercivity components are generally very small (Fig. 2c). All samples are completely demagnetized at temperatures around 540-560 ºC while in some cases a drop of magnetization is noticed at temperatures around 280 ºC. These data confirm the dominance of a low coercivity mineral, most probably magnetite, while some magnetic phase with low Curie temperature may be also present.

3.4 Magnetic susceptibility versus temperature (k-T) curves

Low-field magnetic susceptibility versus temperature experiments (k–T curves) are useful to determine the Curie temperature (T_C) and evaluate the stability of the magnetic carriers upon heating. Thermomagnetic k-T curves have been performed at the University of Montpellier, France. First, a piece of baked clay was crushed in an agate mortar and sieved to collect the 0.4-0.8 mm size fraction. Then k–T curves were

acquired at low-temperature by means of a cryostat apparatus (CS-L) and at high-temperature under Argon by means of a furnace (CS-3) coupled to the KLY-3 Kappabridge instrument (AGICO, Czech Republic). The studied material was first heated from the liquid nitrogen temperature (-194 ºC) to about 650 ºC and cooled down to room temperature. The data were corrected for the empty holder and normalized to the maximum susceptibility. The heating-cooling curves obtained are generally reversible, indicating only minor magnetic mineralogical transformations during heating (Fig. 3). The Curie temperature is estimated to be around 580 ºC suggesting the presence of magnetite, which is in agreement with our previous experiments. Furthermore, these results show that the studied material is thermally stable and suitable for archaeointensity study.

3.5 Hysteresis curves

Hysteresis loops and magnetic moment versus temperature profiles from representative samples were measured at INRIM (Torino, Italy) with a *Lake Shore* 7400 Vibrating Sample Magnetometer (VSM) equipped with a thermo-resistance oven operating in Ar atmosphere. The parameters obtained from the hysteresis curves are plotted in a Day plot (Day et al., 1977) in order to investigate the domain state of the magnetic grains (Fig. 4a). All of the studied samples fall in the pseudo single domain range, indicating the presence of a mixture of SD and MD or SD and SP grains (Dunlop and Carter-Stiglitz, 2006). Further investigation of the grain size was following performed with FORC diagrams.

Thermomagnetic curves of saturation magnetization M_S versus temperature (M_S-T) were also performed for representative samples. Small sample chips of about 50 mg were prepared, and for the same sample M_S-T curves were repeated at

227 increasing maximum temperatures. Each sample was gradually heated at 430 °C and
228 cooled back to room temperature by thermal inertia, while its magnetization was
229 continuously measured during both heating and cooling. Then, for the same sample,
230 the heating-cooling circle was repeated up to 540 °C, and finally up to 650 °C (Fig.
231 4b). Hysteresis loops have also been measured before and after thermal treatments
232 applying a maximum intensity field, H_{max}, equal to 1 T (Fig. 4c).

233 The thermomagnetic curves obtained can offer information about the magnetic
234 mineralogy, thermal stability and grain size of the magnetic carriers but also give
235 evidence about the firing temperatures achieved within the ovens during their use in
236 ancient times. Indeed, reversible changes of magnetic properties should be expected
237 when samples are experimentally heated at temperatures lower (or equal) to those
238 experienced in the past, e.g. during their use at Neolithic times (Hrouda et al., 2003;
239 Carrancho and Villalain, 2011; Spassov and Hus, 2006) while significant differences
240 are expected at higher temperatures. The results obtained show the prevalence of a
241 soft magnetic phase, with Curie (T_C) temperature below 580 °C (Fig. 4b), in good
242 agreement with the results obtained from the IRM, Lowrie experiments and k-T
243 curves. Using the derivative function of heating curves during thermomagnetic
244 analysis, T_C values have been identified between 573 °C and 577 °C, with an average
245 temperature corresponding to 575 ± 2 °C, i.e. near to the Curie point of magnetite. A
246 further confirmation of the dominance of a soft magnetic phase is given by the
247 hysteresis loops that show that the magnetization is almost completely saturated at
248 fields of around 0.3 T (Fig. 4c).

249 Comparison of the thermomagnetic curves obtained at different temperatures
250 shows that the studied material has an almost reversible behavior up to 430 °C.
251 However, when the sample is heated at higher temperatures (e.g. 540 ºC and 650 ºC),

252 the heating and cooling curves show an irreversible behavior, indicating that probably
253 mineralogical changes took place during heating (Fig. 4b, c). This is also confirmed
254 by the hysteresis curves that show a clear increase of the coercive force after heating
255 at 650 ºC compared with the coercive force obtained before heating (Fig. 4c). Such
256 increase is probably caused by mineralogical transformations that have produced a
257 higher coercivity mineral, most probably hematite. The results obtained here suggest
258 that the firing temperatures of the ovens in ancient times were between 430 ºC and
259 540 ºC, in good agreement with the temperatures estimated by the X-ray powder
260 diffraction analysis (Muntoni and Ruggiero, 2013).
261
262 *3.6 First order reversal curves (FORC diagrams)*
263 In order to further characterize the grain size of the samples, first-order reversal curve
264 (FORC) diagrams were measured with a magnetometer (μ-VSM) from Princeton
265 Measurements Corporation at the IPGP-IMPMC Mineral Magnetism Analytical
266 Facility. FORC diagrams were measured with an averaging time of 0.1 s and a
267 saturating field of 1 T. One hundred and fifty FORCs were used to calculate each
268 FORC diagram. They were analyzed with the VARIFORC software (Egli, 2013),
269 using a variable smoothing factor. The variable smoothing considerably reduces the
270 noise levels by applying larger smoothing factors to the background, while preserving
271 the areas along the axes with relatively small smoothing factors.
272 A total of 7 samples from the three ovens were analyzed. The two studied
273 samples from oven PFO-14 show behavior characteristic of stable single-domain
274 grains, with most of the contours closed, and moderate interactions (Fig. 5a) (Roberts
275 et al., 2000). The outermost contours diverge slightly, which could indicate the
276 presence of a small fraction of superparamagnetic (thermally unstable) grains. The

277 coercivity peak is around 20 mT and contours extend as far as 60-70 mT. The two
278 samples from oven PFO-16 are characterized by a peak close to the Hc = 0 axis and
279 very little spreading (Fig. 5b), which seems to indicate the presence of single domain
280 grains, among which some have a relaxation time close to the time of the experiment.
281 Three samples from PFO-17 oven were measured, showing two types of behavior.
282 Sample PFO-17-1 has a FORC diagram very similar to that of PFO-16 (Fig. 5c). The
283 other two samples are characterized by two peaks: one close to the Hc = 0 axis and
284 one further away on the Hc axis, centered at Hc = 13 mT (Fig. 5d), which indicates
285 the presence of stable and viscous single domain grains. The three types of FORC
286 diagrams suggest the presence of very fine grains and little interactions, making these
287 samples ideal candidates for archaeomagnetic analyses.
288
289 **4. Methods and results**
290 *4.1 Magnetic anisotropy*
291 Before the application of the magnetic cleaning, the bulk magnetic
292 susceptibility was measured for all samples. Then, the anisotropy of the magnetic
293 susceptibility (AMS) was investigated in order to examine any possible deviation of
294 the direction of the characteristic remanent magnetization (ChRM) carried by the
295 samples with respect to the direction of the geomagnetic field in the past. All
296 measurements were performed at the ALP palaeomagnetic laboratory with a KLY-3
297 Kappabridge (AGICO). The low field bulk magnetic susceptibility varies from 1.68 x
298 10^{-3} to 14.96 x 10^{-3} SI, with the higher values coming from oven PFO-17 (Table 1).
299 The degree of AMS (P_{AMS}) (Jelinek, 1981) is very low and varies between 1.002 <
300 P_{AMS} < 1.023 with mean value 1.008 for oven PFO-14, 1.007 for PFO-16 and 1.005
301 for PFO-17 (Table 1). The anisotropy results obtained here are in agreement with

302 those from previous studies on prehistoric baked clays (e.g. Kovacheva et al., 2009)
303 and confirm that the anisotropy of baked clays from ovens and fire places is
304 negligible, in contrary to the results from brick kilns or ceramics that are usually
305 highly anisotropic (Chauvin et al., 2000; Hus et al., 2002; Tema, 2009).
306
307 *4.2 Archaeomagnetic direction determination*
308 The natural remanent magnetization (NRM) of 39 samples was first measured
309 with a JR6 spinner magnetometer at the ALP palaeomagnetic laboratory (Peveragno,
310 Italy). Subsequently, all samples were demagnetized applying stepwise alternating
311 field (AF) up to 80 mT with a ASC-D 2000 equipment. The plastic boxes used for
312 sampling prevented the application of systematic thermal demagnetization
313 procedures. Almost all samples are demagnetized in relatively low AF fields, around
314 40-60 mT, confirming the presence of a low coercivity magnetic mineral.
315 Demagnetization results are illustrated in orthogonal vector components diagrams
316 (Zijderveld, 1967) and the characteristic remanent magnetization (ChRM) for each
317 sample has been easily isolated (Fig. 6a).
318 We determined the ChRM by means of principal component analysis
319 (Kirschvink, 1980), averaged the directions thus obtained by oven, and calculated the
320 statistical parameters assuming a Fisherian Distribution (Fisher, 1953). All directions
321 at sample level are reported in Table 1, together with the Maximum Angular
322 Deviation values (MAD). The directions obtained from the three ovens are very
323 similar with each other: D= 357.0º, I=60.9º, α_{95}= 2.0, k= 448 for oven PFO-14,
324 D=357.0º, I=57.7º, α_{95}= 2.4, k= 450 for oven PFO-16 and D=352.8º, I=57.9º, α_{95}=
325 2.1, k=611 for oven PFO-17 (Fig. 6b and Table 1). All mean directions are

326 characterized by small α_{95} angles of confidence and high values of precision
327 parameter k.
328
329 *4.3 Archaeomagnetic intensity determination*
330 Absolute intensity determinations of a collection of samples from the three
331 ovens were carried out at the University of Montpellier with the multispecimen
332 protocol. The multispecimen technique offers a viable alternative to the classical
333 Thellier-Thellier method of absolute palaeointensity determination, having a great
334 potential to improve and simplify the palaeointensity measurements (Biggin and
335 Poidras, 2006; Dekkers and Böhnel, 2006; Fabian and Leonhardt, 2010). The
336 experiments were performed with a prototype of a very fast-heating infrared furnace
337 developed in Montpellier (FURéMAG, patent #1256194), which has the advantage of
338 heating samples of 10-cc-standard volume very quickly and uniformly. A total of 21
339 samples, 7 from each oven, have been studied with the MSP-DSC protocol (Fabian
340 and Leonhardt 2010). Thanks to the prototype FURéMAG furnace, a precise magnetic
341 induction field, perfectly controlled in 3D with a measured precision better than 1°
342 was applied to each sample during the heating (and cooling). The heating temperature
343 for the partial thermal remanent magnetization (pTRM) acquisition was chosen to be
344 320 °C for all samples; this temperature is considered high enough to involve a
345 sufficient fraction of the TRM (at least 20 %) but sufficiently low to avoid chemical
346 alteration. In the MSP protocol, the pTRM is imparted along the NRM direction, thus
347 no anisotropy correction is necessary. Moreover, the AMS results previously
348 discussed showed that the Portonovo samples are characterized by a very weak
349 anisotropy that would not effect the pTRM direction imparted during the laboratory

heatings. In multispecimen protocol, cooling rate correction is also not required (Fanjat, 2012).

A set of strict criteria was adopted to select the individual MSP data and screen out those of poor technical quality. The applied criteria are essentially based on three considerations.

1. The fraction of unblocked NRM during the heatings must be between 20% and 80% of the total NRM. In this interval, the fraction is large enough to be accurately measured and well below a total TRM.
2. The maximum angle between the NRM left after the pTRM acquisition and the total NRM is fixed at 10°.
3. The relative alteration error ε_{alt} (see equation 19 in Fabian and Leonhardt, 2010) must be lower than 10%.

For the three ovens, all the rejected samples were discarded from further analysis due to a significant alteration error (greater than 10%). The regression analysis remains possible for oven PFO-14 and for oven PFO-16, with 4 samples selected, while it is unfortunately precluded for oven PFO-17 since only 3 samples were selected. The intensity values obtained for ovens PFO-14 and PFO-16 are very similar, whatever the protocol involved (DB, FC, or DSC) in the archaeointensity determination (for details about the various protocols, see Fabian and Leonhardt, 2010) and whatever the value of alpha parameter (see Table 2 and Figure 7). As recommended by Fabian and Leonhardt (2010) our preferred archaeointensity estimations are those given by the MSP-DSC protocol with the alpha parameter equal to 0.5, and they are 28.2 ± 1.0 µT and 26.7 ± 0.9 µT for ovens PFO-14 and PFO-16, respectively. These results show very similar intensities for the two ovens suggesting that they were used and abandoned in short time periods one after the other.

5. New data and the geomagnetic field in southern Europe during the Neolithic period

The new archaeomagnetic data presented in this study are the first full geomagnetic field results available up to now in Italy for the Neolithic period. Tema et al. (2006) presented two directional data from baked clay hearths excavated at the Mesolithic site of Laghetti del Crestoso (Brescia, northern Italy). Nevertheless, these results were obtained based only on NRM measurements and zero field viscosity tests and they are characterized by large α_{95} confidence angles (α_{95}= 11.6° and 17.7° respectively). Even though they give some indication about the Earth's magnetic field direction in Italy during the prehistoric time, they cannot be considered reliable enough for secular variation reconstructions. More recently, Kapper et al. (2014) studied different levels of anthropogenic burnt sediments in the Riparo Gaban rock shelter (Trento, northern Italy) and obtained seven new directional results for the time period spanning from 5000 BC to 2300 BC. These results are also characterized by relatively large α_{95} angles, varying from 5° to 13.3°, probably because of the low combustion temperatures of the sediments and possible disturbances caused by bioturbation and anthropogenic factors (Kapper et al., 2014). No intensity data from Italian artifacts with ages older than the last two millennia are available before now (Tema, 2011).

Archaeomagnetic data from the prehistoric period are also extremely scarce in the whole of central Europe. To our knowledge, only two directional data from Germany and few data from Hungary are available for the 6000-4000 BC period. Schnepp et al. (2004) presented the archaeomagnetic direction of an oven excavated at Untergaiching (southern Germany) and Schnepp and Lanos (2005) obtained one

more directional result from Germany by studying the archaeomagnetic direction of an oven excavated at Bernstorf, close to Kranzberg in southern Germany, with an age between 5526 BC and 5373 BC. Márton (2009) published a set of prehistoric archaeomagnetic directions from different sites in Hungary, with ^{14}C ages ranging from 5500 BC to 4490 BC (no age errors are reported in the publication). Regarding the archaeomagnetic intensity data, again almost no data are available, with the exception of few archaeointensity records from Czech Republic reported in the early work of Bucha (1967). Conversely, an extended dataset of both directional and intensity data is available for Eastern Europe, mainly coming from the Balkan Peninsula (Tema and Kondopoulou, 2011). Bulgaria has one of the richest archaeomagnetic records in Europe that covers almost continuously the last 8000 years (Kovacheva et al., 2009; 2014) while an important number of directional (De Marco et al., 2014) and intensity data (De Marco et al., 2008) are also available for Greece. Few data from prehistoric times are also available from other countries of Eastern Europe such as Serbia and Romania (Brown et al., 2015, Geomagia50.v3.1 database).

The new full geomagnetic field results presented here are compared with published data from Italy, central Europe and Balkan Peninsula available for the 6000-4000 BC period (Fig. 8). Data from the Balkan Peninsula (Tema and Kondopoulou, 2011) have been updated with some recently published data from Bulgaria (Kovacheva et al., 2014) and Greece (Fanjat et al., 2013), taken from the updated Geomagia50.v3.1 database. For comparison, all data have been relocated at Viterbo (42.45 ºN, 12.03 ºE), situated in central Italy (around 70 km from Rome), which was chosen as the optimum reference point for archaeomagnetic studies in Italy (Lanza and Zanella, 2003; Tema et al., 2006; 2010). The comparison shows that the

directions obtained from the Portonovo ovens are in very good agreement with the data from Germany and Hungary from the same time period (Fig. 8a, b). Good agreement can also be observed with the directional data from the Balkan Peninsula. As far as the intensity data are concerned, Portonovo results clearly show a low intensity value around 28±1 μT. This low intensity seems to be confirmed by some data from Bulgaria that show intensity values of around 30-35 μT, even though some dispersion in the published data can be noticed around 5500 BC, with intensities as high as 45 μT (Fig. 8c).

The new data have been also compared with the predictions of the CALS10k.1b (Korte et al., 2011), the pfm9k.1a (Nilson et al., 2014) and the SCHA.DIF.14k (Pavon-Carrasco et al., 2014) global geomagnetic field models that are the most recently published models that cover the Neolithic period. The Portonovo directions are in very good agreement with the models, while the Portonovo intensity is lower than the models predictions (Fig. 8). Actually, both pfm9k.1a and SCHA.DIF.14k models tend to show an important decrease in intensity for the period around 5500 BC. However, the model predictions show much smoother variations with respect to those indicated by the archaeomagnetic data, probably influenced by the sedimentary records included in the reference dataset of some models for the BC periods and/or the often the important dispersion of the reference data. This clearly highlights the importance of new, high quality data that can contribute to improvement of the models' resolution.

6. Discussion and conclusions

The material collected from the Neolithic ovens of Portonovo, even if very fragile and baked at relatively low temperatures (<500 ºC), has been shown to be a

reliable recorder of the Earth's magnetic field in the past. Both directional and intensity results obtained are of high quality, offering the first full geomagnetic field vector data for Neolithic period in Italy. The directions and intensities recorded by the three ovens are very similar, suggesting that the ovens were in use and abandoned almost at the same time or in time periods very close one to the other, when the geomagnetic field was almost the same. This is in very good agreement with the archaeological findings suggesting that each oven was in use for a very short period of time (few years or decades), while the whole site was occupied for just few centuries.

Taking into account the very well determined geomagnetic field vector, with directions accompanied by low α_{95} angles of confidence and intensities characterized by small confidence intervals, we have tried to further investigate the possibility of reconstructing the chronological sequence of the construction and abandonment of the three studied ovens by archaeomagnetic dating. We have therefore compared the declination, inclination and intensity determined for each oven with the predictions of the SCHA.DIF.14k European geomagnetic field model (Pavón-Carrasco et al., 2014), that is only based on archaeomagnetic and volcanic rock data and therefore offers one of the most reliable global geomagnetic field models for the prehistoric period. For oven PFO-17, dating was performed based only on declination and inclination. Such comparison shows that at 95 % of probability the last firing of each oven occurred at: 5479-5403 BC for oven PFO-14 (or 5463-5429 BC at 65% of probability), 5472-5395 BC for oven PFO-16 (or 5455-5423 BC at 65 % of probability) and 5522-5359 BC for oven PFO-17 (or 5503-5405 BC at 65% of probability). Dating obtained for oven PFO-17 based only on the direction shows a quite wide time interval, demonstrating that the contribution of archaeointensity is very important for restricting the archaeomagnetic dating results. Nevertheless, the dating results of all ovens are in

475 very good agreement with the dating of the site based on archaeological evidence and
476 available ^{14}C dating.

477 Archaeomagnetic dating results suggest that the PFO-17 oven is most likely to
478 belong to a separate group of ovens and it was damaged and abandoned before ovens
479 PFO-14 and PFO-16. On the other hand, ovens PFO-14 and PFO-16 are most
480 probably abandoned at the same time or with very short time difference in presence of
481 actually almost the same ambient geomagnetic field. This hypothesis seems to be also
482 supported by the vicinity of the two ovens, and probably when one was damaged by
483 repeated use, the other was built just attached to the previous one. Of course this
484 interpretation should be used with caution and integrated with other archaeological
485 evidence, as the wide dating interval obtained for oven PFO-17 and the overlapping of
486 the obtained archaeomagnetic dating for PFO-14 and PFO-16 ovens caused by their
487 statistically similar directions and intensities, does not allow more precise
488 chronological reconstruction. Moreover, archaeomagnetic dating always refers to the
489 last firing of the ovens, usually corresponding to their abandonment but it can not
490 offer information about the date of construction or period of use of the structures that
491 could have occurred much earlier.

492 The new full geomagnetic field vector results presented here aim to offer new
493 data about the Earth's magnetic field in Italy during the Neolithic period and enrich
494 the available global dataset that is still poor for the prehistoric period. The clear, well
495 defined, low intensity values obtained here suggest that the intensity of the Earth's
496 magnetic field around 5500 BC was almost 20 μT lower that the today's field in Italy.
497 Such low intensity seems to be an interesting feature of the field in Neolithic period,
498 noticed also in the Balkan Peninsula, and it should be further investigated by
499 obtaining new high quality data from Europe from the same chronological period.

Undoubtedly, obtaining new data from well-dated archaeological material is also a key issue for improving the resolution of geomagnetic field models in the past, in order to identify the fine features and rapid geomagnetic field variations, as well as extending reliable archaeomagnetic dating in prehistoric periods.

Acknowledgments

This study was partially financed by the PHC Galileo 2012-2013 exchange program. The Géosciences Montpellier was supported by a grant from the CNRS-PNP. The FUReMAG rapid furnace construction was supported by the French National Agency for Research (ANR-12-BS06-0015). Cathy Batt is highly acknowledged for improving the English style and Giorgio Bertotti is sincerely thanked for discussion and suggestions on the manuscript. Elisabeth Schnepp and an anonymous reviewer are acknowledged for their comments on the manuscript.

516

517 **References**

518 Biggin, A.J., Poidras, T., 2006. First-order symmetry of weak-field partial
519 thermoremanence in multi-domain ferromagnetic grains. 1. Experimental evidence
520 and physical implications. Earth and Planetary Science Letters, 245(1-2), 438–453.
521 doi:10.1016/j.epsl.2006.02.035.

522

523 Brown, M.C., Donadini, F., Korte, M., Nilsson, A., Korhonen, K., Lodge, A.,
524 Lengyel, S.N., Constable, C.G., 2015. GEOMAGIA50.v3: 1. General structure and
525 modifications to the archeological and volcanic database. Earth Planets Space, 67:83,
526 doi:10.1186/s40623-015-0232-0.

527

528 Bucha, V., 1967. Intensity of the Earth magnetic field during archeological times in
529 Czechoslovachia. Archaeometry, 10, 12-22, doi: 0.1111/j.1475-4754.1967.tb00608.x.

530

531 Carrancho, A., Villalaín, J.J., 2011. Different mechanisms of magnetization recorded
532 in experimental fires: archaeomagnetic implications. Earth and Planetary Science
533 Letters, 312, 176-187.

534

535 Chauvin, A., Garcia, Y., Lanos Ph., Laubenheimer, F., 2000. Palaeointensity of the
536 geomagnetic field recovered on archaeomagnetic sites from France. Physics Earth
537 Planetary Interiors, 120, 111-136.

538

539 Conati Barbaro, C., 2013. Cooking, working and burying in Ancient Neolithic: The
540 ovens of Portonovo (Marche, Italy)), with contributions by Acquafredda P., Catalano

P., Celant A., Di Giannantonio S., Lelli R., Muntoni I.M., Pallara M., Ruggero G. Origini, XXXV, 31-82.

Day, R., Fuller, M., Schmidt, V.A., 1977. Hysteresis properties of titanomagnetites: Grain size and composition dependence. Physics Earth and Planetary Interiors, 13, 260-267.

De Marco, E., Spatharas, V., Gómez-Paccard, M., Chauvin, A., Kondopoulou D., 2008. New archaeointensity results from archaeological sites and variation of the geomagnetic field intensity for the last 7 millennia in Greece. Phys. Chem. Earth, 33, 578-595.

De Marco, E., Tema, E., Lanos, Ph., Kondopoulou, D., 2014. An updated catalogue of Greek archaeomagnetic data for the last 4500 years and a directional secular variation curve. Stud. Geophys. Geod., 58, 121-147, doi: 10.1007/s11200-013-0910-y.

Dekkers, M. J., Böhnel, H. N., 2006. Reliable absolute palaeointensities independent of magnetic domain state. Earth and Planetary Science Letters, 248 (1-2), 508–517, doi: 10.1016/j.epsl.2006.05.040.

Dunlop, D.J., Carteer-Stiglitz, B., 2006. Day plots of mixtures of superparamagnetic, single-domain, pseudosingle-domain, and multidomain magnetites. Journal of Geophysical Research, 111, B12S09, doi: 10.1029/2006JB004499.

565 Egli, R. 2013. VARIFORC: An optimized protocol for calculating non-regular first-
566 order reversal curve (FORC) diagrams. Global and Planetary Change, 110, 302-320.
567 http://dx.doi.org/10.1016/j.gloplacha.2013.08.003.
568
569 Fabian, K., Leonhardt R., 2010. Multiple-specimen absolute paleointensity
570 determination: an optimal protocol including pTRM normalization, domain-state
571 correction, and alteration test. Earth Planetary Science Letters, 207, 84-94.
572
573 Fanjat G., 2012. Les fluctuations du champ magnétique terrestre : des variations
574 séculaires récentes aux renversements. *Available online at https://tel.archives-*
575 *ouvertes.fr/tel-00719380.*
576
577 Fanjat, G., Aidona, E., Kondopoulou, D., Camps, P., Rathossi, C., Poidras, T., 2013.
578 Archeointensities in Greece during the Neolithic period: New insights into material
579 selection and secular variation curve. Phys. Earth Planet. Int., 215, 29-42, doi:
580 10.1016/j.pepi.2012.10.011.
581
582 Fisher R.A., 1953. Dispersion on a sphere. Proceedings of Royal Society, London,
583 pp.295.
584
585 Jelinek, V., 1981. Characterization of the magnetic fabric of rocks. Tectonophysics,
586 79, 63-67.
587

588 Hrouda, F. 2003. Indices for numerical characterization of the alteration processes of
589 magnetic minerals taking place during investigation of temperature variation of
590 magnetic susceptibility. Studia Geophysica et Geodaetica, 47, 847-861.
591
592 Hus, J., Ech-Chakrouni, S., Jordanova, D., 2002. Origin of magnetic fabric in bricks:
593 its implications in archaeomagnetism. Phys. Chem. Earth, 27, 1319-1331.
594
595 Kapper, L., Anesin, D., Donadini, F., Angelucci, D., Cavulli, F., Pedrotti, A., Hirt, A.,
596 2014. Linking site formation processes to magnetic properties. Rock- and
597 Archeomagnetic analysis of the combustion levels at Riparo Gaban, Italy. Journal of
598 Archaeological Science, 41, 836-855.
599
600 Kirschvink J.L., 1980. The least-square line and plane and the analysis of
601 palaeomagnetic data. Geophys. J. Astron. Soc., 62, 699-718.
602
603 Korte, M., Constable, C., Donadini, F., Holme, R., 2011. Reconstructing the Holocene
604 geomagnetic field. Earth Planetary Science Letters, 312, 3-4, 497-505, doi:
605 10.1016/j.epsl.2011.10.031.
606
607 Kovacheva, M., Chauvin, A., Jordanova, N., Lanos, Ph., Karloukovski, V., 2009.
608 Remanence anisotropy effect on the palaeointensity results obtained from various
609 archaeological materials, excluding pottery. Earth Planets Space, 61, 711-732.
610
611 Kovacheva, M., Kostadinova-Avramova, M., Jordanova, N., Lanos, Ph., Boyadziev,
612 Y., 2014. Extended and Revised Archaeomagnetic Database and secular variation

613 curves from Bulgaria for the Last Eight Millennia. Physics Earth and Planetary
614 Interiors, 236, 79-94.
615
616 Lanza, R., Zanella, E., 2003. Palaeomagnetic secular variation at Vulcano (Aeolian
617 Islands) during the last 135 kyr. Earth Planet. Sci. Lett., 213, 321-336.
618
619 Lowrie, W., 1990. Identification of ferromagnetic minerals in a rock by coercivity and
620 unblocking temperature properties. Geophys. Res. Lett., 17, 159-162.
621
622 Márton, P., 2009. Prehistorical archeomangetic directions from Hungary in
623 comparison with those from South-eastern Europe. Earth Planets Space, 61, 1351-
624 1356.
625
626 Muntoni, I.M., Ruggiero, G., 2013. Estimating the Firing temperatures of
627 pyrotechnological processes in Neolithic site of Portonovo. Origini, XXXV, 52-56.
628
629 Nilsson, A., Holme, R., Korte, M., Suttie, N., Hill, M., 2014. Reconstructing
630 Holocene geomagnetic field variation: new methods, models and implications.
631 Geophysical Journal International, 198, 1, 229-248.
632
633 Pavón-Carrasco, F.J., Osete, M.L., Torta, J.M., De Santis, A., 2014. A geomagnetic
634 field model for the Holocene based on archaeomagnetic and lava flow data. Earth
635 Planetary Science Letters, 388, 98 - 109.
636

637 Prévot, M., 1981. Some aspects f magnetic viscosity in subaerial and submarine
638 volcanic rocks. Geophys. J. R. Astr. Soc., 66, 169-192.
639
640 Reimer, P.J., Baillie, M.G.L.,Bard, E., Bayliss, A., Beck, J.W., Bertrand, C.,
641 Blackwell, P.G., Buck, C.E., Burr, G., Cutler, K.B., Damon, P.E., Edwards, R.L.,
642 Fairbanks, R.G., Friedrich, M., Guilderson, T.P., Hughen, K.A., Kromer, B.,
643 McCormac, F.G., Manning, S., Bronk Ramsey, C., Reimer, R.W., Remmele, S.,
644 Southon, R.J., Stuiver, M., Talamo, S., Taylor, F.W., van der Plicht, J.,
645 Weyhenmeyer, C.E., 2004. IntCal04 Terrestrial radiocarbon age calibration, 0-26 Cal
646 Kyr BP. Radiocarbon, 46 (3), 1029-1058.
647
648 Reimer, P.J., Baillie, M.G.L., Bard, E., Bayliss, A., Beck, J.W., Blackwell, P.G.,
649 Bronk Ramsey, C., Buck, C.E., Burr, G.S., Edwards, R.L., Friedrich, M., Grootes,
650 P.M., Guilderson, T.P., Hajdas, I., Heaton, T.J., Hogg, A.G., Hughen, K.A., Kaiser,
651 K.F., Kromer, B., McCormac, F.G., Manning, S.W., Reimer, R.W., Richards, D.A.,
652 Southon, J.R., Talamo, S., Turney, C.S. M., van der Plicht, J., Weyhenmeyer, C.E.
653 2009. IntCal09 and Marine09 radiocarbon age calibration curves, 0-50,000 years cal
654 BP. Radiocarbon, 51(4), 1111-1150.
655
656 Roberts, A. P., Pike, C. R. and Verosub, K. L., 2000. First order reversal curve
657 diagrams: a new tool for characterizing the magnetic properties of natural samples.
658 Journal of Geophysical Research , 105, 28461-28475.
659
660 Schnepp, E., Lanos, Ph., 2005. Archaeomagnetic secular variation in Germany during
661 the past 2500 years. Geophysical Journal International, 163, 479-490.

662

663 Schnepp, E., Pucher, R., Reinders, J., Hambach, U., Soffel, H., Hedley, I., 2004. A
664 German catalogue of archaeomagnetic data. Geophysical Journal International, 157,
665 64-78, doi: 10.1111/j.1365-246X.2004.02163.x.

666

667 Spassov, S., Hus, J., 2006. Estimating baking temperatures in a Roman pottery kiln by
668 rock magnetic properties: implications of thermochemical alteration on
669 archaeointensity determinations. Geophysical Journal International, 167, 592-604.

670

671 Tema, E., Kondopoulou, D., 2011. Secular variation of the Earth's magnetic field in
672 the Balkan region during the last eight millennia based on archaeomagnetic data.
673 Geophysical Journal International, 186, 2, 603-614, doi: 10.1111/j.1365-
674 246X.2011.05088.x

675

676 Tema, E., Goguitchaichvili, A., Camps P., 2010. Archeointensity determination from
677 Italy: new data and Earth's magnetic field strength variation over the past three
678 millennia. Geophysical Journal International, 180, 596-608, doi: 10.1111/j.1365-
679 246X.2009.04455.x

680

681 Tema, E., Hedley, I., Lanos, Ph., 2006. Archaeomagnetism in Italy: A compilation of
682 data including new results and a preliminary Italian Secular Variation curve.
683 Geophysical Journal International, 167, 1160-1171.

684

685 Tema, E., 2009. Estimate of the magnetic anisotropy effect on the archaeomagnetic
686 inclination of ancient bricks. Physics of Earth and Planetary Interiors, 176, 213-223,
687 doi: 10.1016/j.pepi.2009.05.007.
688
689 Tema, E., 2011. Archaeomagnetic Research in Italy: Recent achievements and future
690 perspectives. In: The Earth's Magnetic Interior, IAGA Special Sopron Book Series,
691 Volume 1, Chapter 15, pp. 213-233. Eds: Petrovsky, E., Herrero-Bervera, E.,
692 Harinarayana, T., Ivers, D., Springer, doi: 10.1007/978-94-007-0323-0_15.
693
694 Thellier, E., Thellier, O., 1944. Recherches géomagnetiques sur les coulees
695 volcaniques d'Auvergne. Ann. Geophys., 1, 37–52.
696
697 Zijderveld, J., 1967. AC demagnetization of rocks: analysis of results. In: Collinson,
698 D., Creer, K., Runcorn, S. (Eds.), Methods in Paleomagnetism. Elsevier, New York,
699 pp. 254-256.
700

Figures captions

Fig. 1. a) Map of Italy with the location of the Portonovo archaeological site; b-c) General view of the excavated ovens; d) Photo of the PFO17 oven; e) General view of the PFO14, PFO16 and PFO16 ovens, sampled for archaeomagnetic analysis.

Fig. 2. a) Histograms of the viscosity index (%) calculated for the three ovens; b) Normalized IRM acquisition curves up to 1.6 T for representative samples from the three ovens; c) Stepwise thermal demagnetization of three IRM components following Lowrie (1990). Symbols: dot= Soft- (0.1 T); diamond= Medium- (0.5 T); square= Hard- (1.6 T) coercivity component.

Fig. 3. Low-field susceptibility versus temperature curves measured under air atmosphere (k-T curves) for a representative sample from oven PFO17. Susceptibility values are normalized to the maximum susceptibility. The heating curve is in red, the cooling curve is in blue.

Fig. 4. a) Day plot obtained from the hysteresis curves of representative specimens from the three ovens. The SD-MD and SD-SP mixing lines are calculations for magnetite from Dunlop and Carter-Stiglitz (2006). Numbers along curves are volume fractions of the soft component (SP or MD) in mixtures with SD grains. All the data plot on the PSD range; b) Thermomagnetic profiles (M-T) obtained for the PFO17a sample after subsequent heating from room temperature up to 430 °C (left), 540 °C (middle), and 650 °C (right). All heating-cooling curves have been normalized to the initial magnetization at room temperature, before any treatment; c) Hysteresis curves obtained for the same PFO17a sample, before (black line) and after treatment at 430

°C (red), 540 °C (green) and 650 °C (blue). The inset shows the behavior of the cycles around the origin of the graphs.

Fig. 5. FORC diagrams obtained from samples a) PFO14-1; b) PFO16-1; c) PFO17-1 and d) PFO17-3. Each FORC diagram is calculated from 150 FORCs measured with an averaging time of 0.1s. Note that the horizontal and vertical scales are the same for the four diagrams.

Fig. 6a.) Stepwise thermal demagnetization results from representative samples from the PFO-14 (left), PFO-16 (middle) and PFO-17 (left) ovens illustrated as Zijderveld plots. Symbols: full dots = declination; open dots = apparent inclination; b) Equal area projections of the ChRM directions at sample level for the three ovens. The big dot represents the mean value calculated for each oven according to Fisher statistics.

Fig. 7. Multi-specimen (MSP) archaeointensity determinations for a) and b) oven PFO14 and c) and d) oven PFO16. Closed (open) symbols represent data used (rejected) in the robust regression of the responses in Q parameters on the predictors in magnetic field B. The MSP-BD and MSP-FC data and fitting lines are represented with magenta and blue lines, respectively. For MSP-DSC plots (red lines), data and fitting lines are calculated with $\alpha = 0.5$. The dashed lines are the 65% confidence intervals on the best fitting lines.

Fig. 8. The new declination (top), inclination (middle) and intensity (bottom) data obtained in this study plotted together with available literature data from Italy, central Europe and Balkan Peninsula for the 6000-4000 BC period. The SV curves calculated

751 from the pfm9k.1a, CALS10K.1b and SCHA.DIF.14k global geomagnetic field
752 models have been also plotted for comparison.
753

754

755 **Tables**

756 Table 1. Archaeomagnetic results. Columns: Sample; Natural Remanent
757 Magnetization; Bulk susceptibility; $P_{AMS:}$ degree of the Anisotropy of Magnetic
758 Susceptibility; Declination (º); Inclination (º); MAD: Maximum Angular Deviation;
759 Mean direction: N= number of independently oriented samples; D_m= mean
760 declination; I_m= mean inclination; α_{95}= 95% semi-angle of confidence; k= precision
761 parameter according to Fisher (1953).

762

763 Table 2. Archaeointensity results for ovens PFO-14, PFO-16 and PFO-17.
764 MSP archaeointensity values are estimated by the zero-crossing point of the Robust
765 linear regression on the Q parameters obtained with the MSP-DB protocol (Dekker
766 and Bohnel, 2006), fraction correction (MSP-FC) or domain state correction protocols
767 (Fabian and Leonhardt, 2010) as function of the laboratory field. R-squared is the
768 coefficient of determination indicating how well data fit the model. RMSE is the root
769 mean squared error for the fitting line.

770

771

772

773

774

775

776

777 Fig. 1

778

779

780

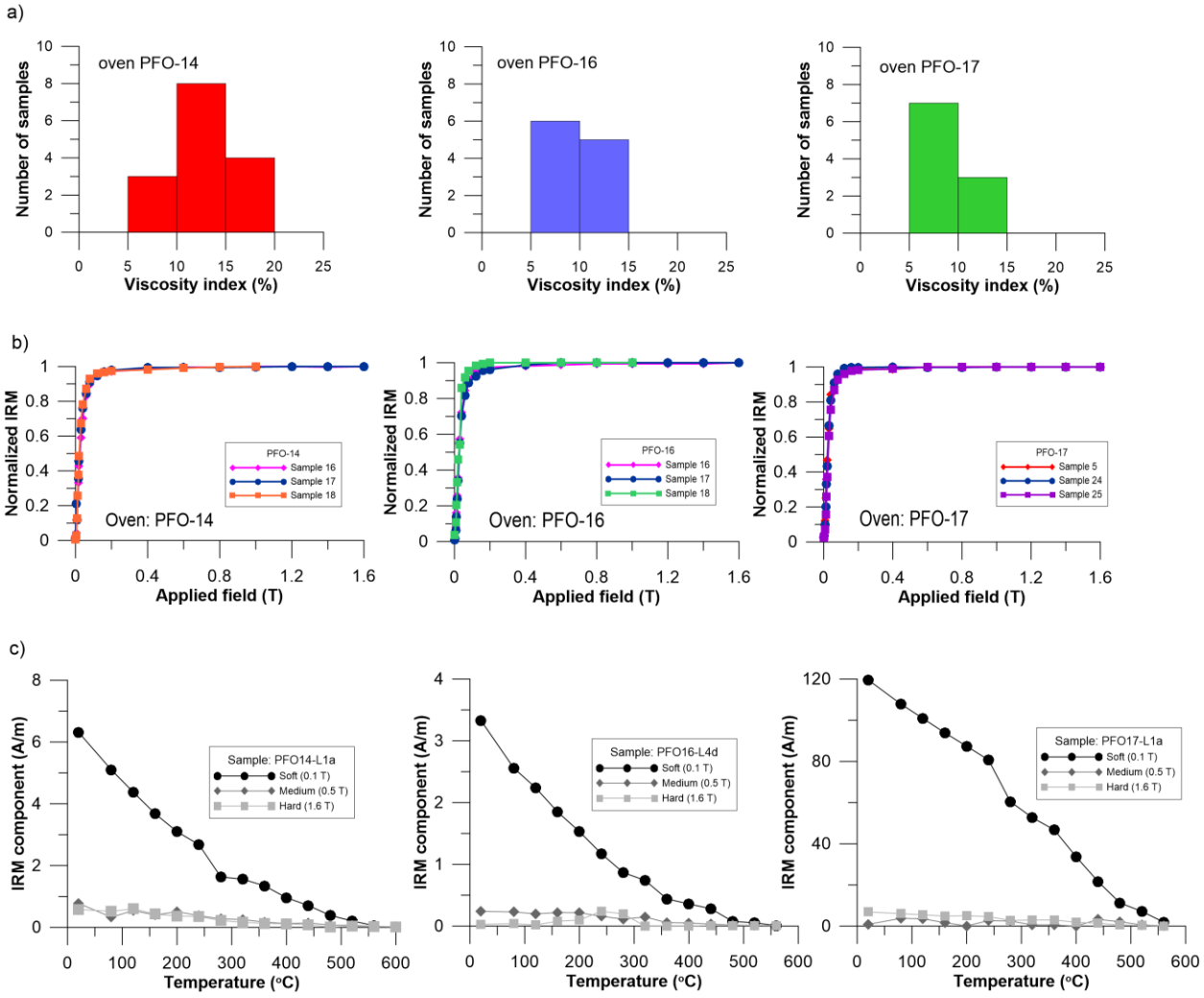
a)
oven PFO-14
oven PFO-16
oven PFO-17
Number of samples
Viscosity index (%)
b)
Normalized IRM
Applied field (T)
Oven: PFO-14
Oven: PFO-16
Oven: PFO-17
PFO-14
Sample 16
Sample 17
Sample 18
PFO-16
Sample 16
Sample 17
Sample 18
PFO-17
Sample 5
Sample 24
Sample 25
c)
IRM component (A/m)
Temperature (°C)
Sample: PFO14-L1a
Sample: PFO16-L4d
Sample: PFO17-L1a
Soft (0.1 T)
Medium (0.5 T)
Hard (1.6 T)

Fig. 2

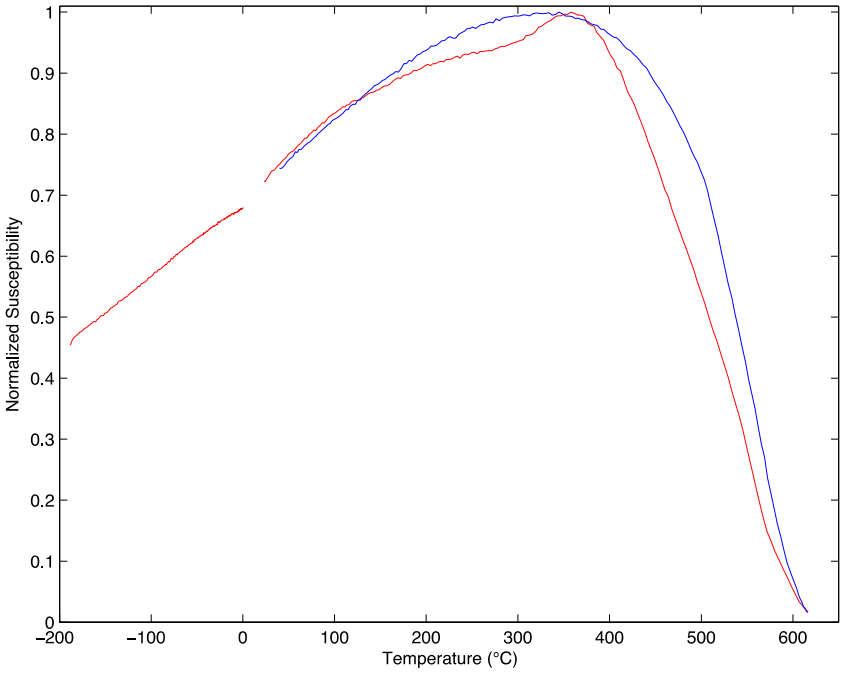
Normalized Susceptibility
Temperature (°C)
0
0.1
0.2
0.3
0.4
0.5
0.6
0.7
0.8
0.9
1
−200
−100
0
100
200
300
400
500
600

Fig. 3

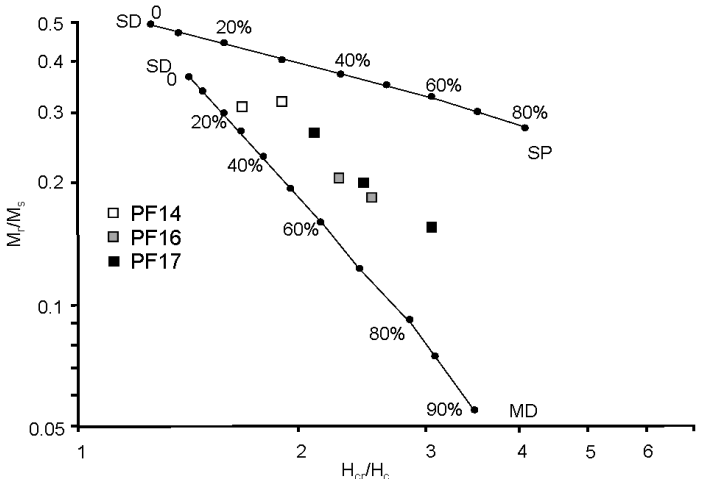
SD
0
20%
40%
60%
80%
SP
SD
0
20%
40%
60%
80%
90%
MD
PF14
PF16
PF17
M_r/M_s
H_{cr}/H_c

(a)

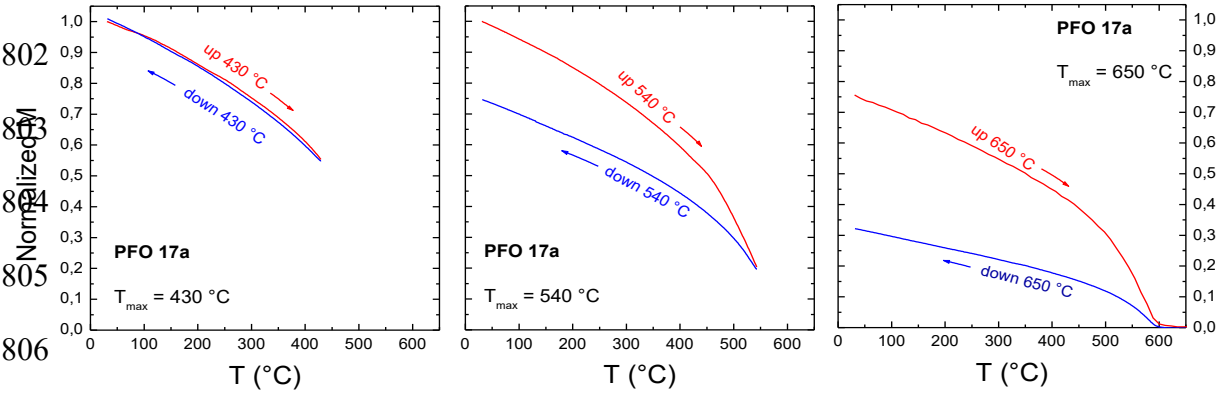
Normalized M
up 430 °C
down 430 °C
PFO 17a
T_{max} = 430 °C
up 540 °C
down 540 °C
PFO 17a
T_{max} = 540 °C
PFO 17a
T_{max} = 650 °C
up 650 °C
down 650 °C
T (°C)
T (°C)
T (°C)

(b)

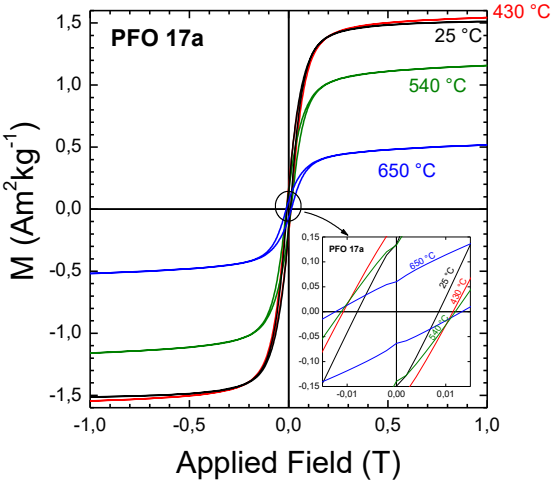
PFO 17a
430 °C
25 °C
540 °C
650 °C
M (Am^2kg^{-1})
Applied Field (T)

(c)

Fig. 4

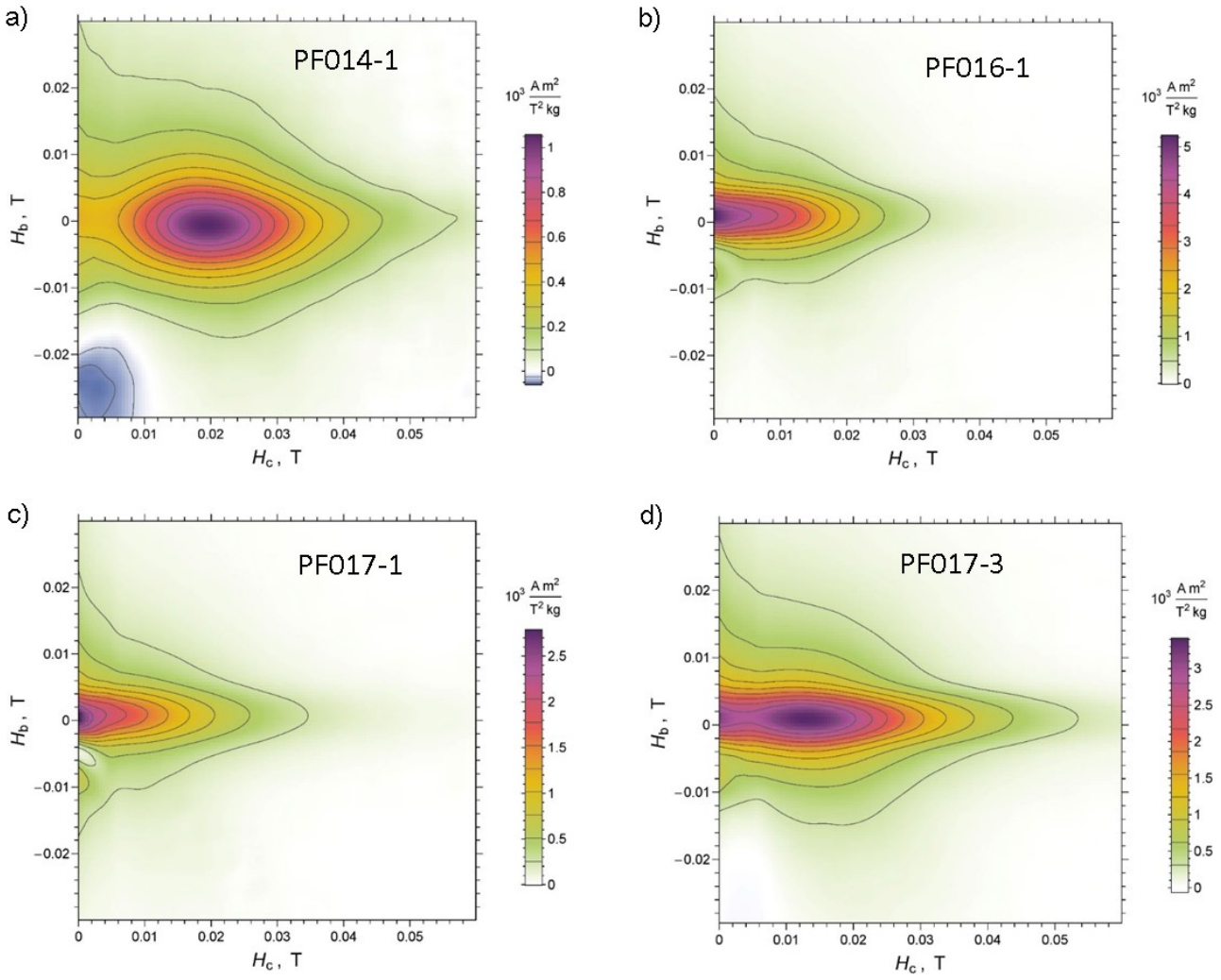

Fig. 5

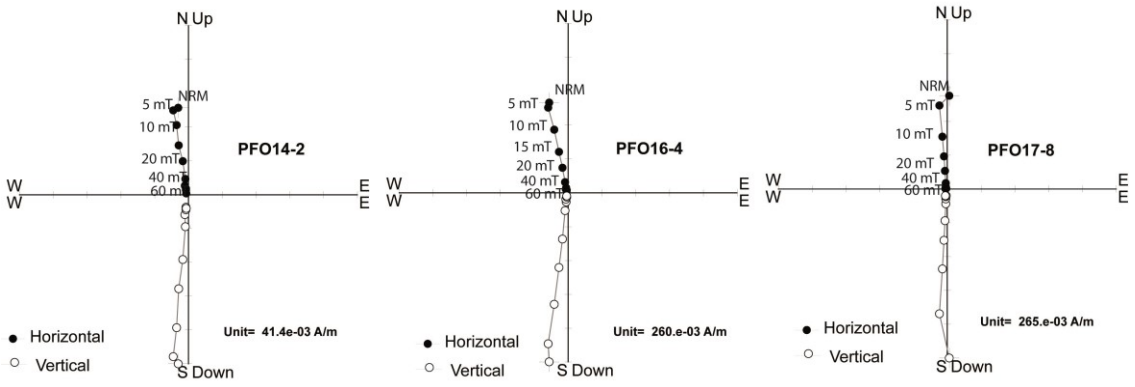
N Up
NRM
5 mT
10 mT
20 mT
40 mT
60 mT
PFO14-2
W
E
S Down
Horizontal
Vertical
Unit= 41.4e-03 A/m
N Up
NRM
5 mT
10 mT
15 mT
20 mT
40 mT
60 mT
PFO16-4
W
E
S Down
Horizontal
Vertical
Unit= 260.e-03 A/m
N Up
NRM
5 mT
10 mT
20 mT
40 mT
60 mT
PFO17-8
W
E
S Down
Horizontal
Vertical
Unit= 265.e-03 A/m

(a)

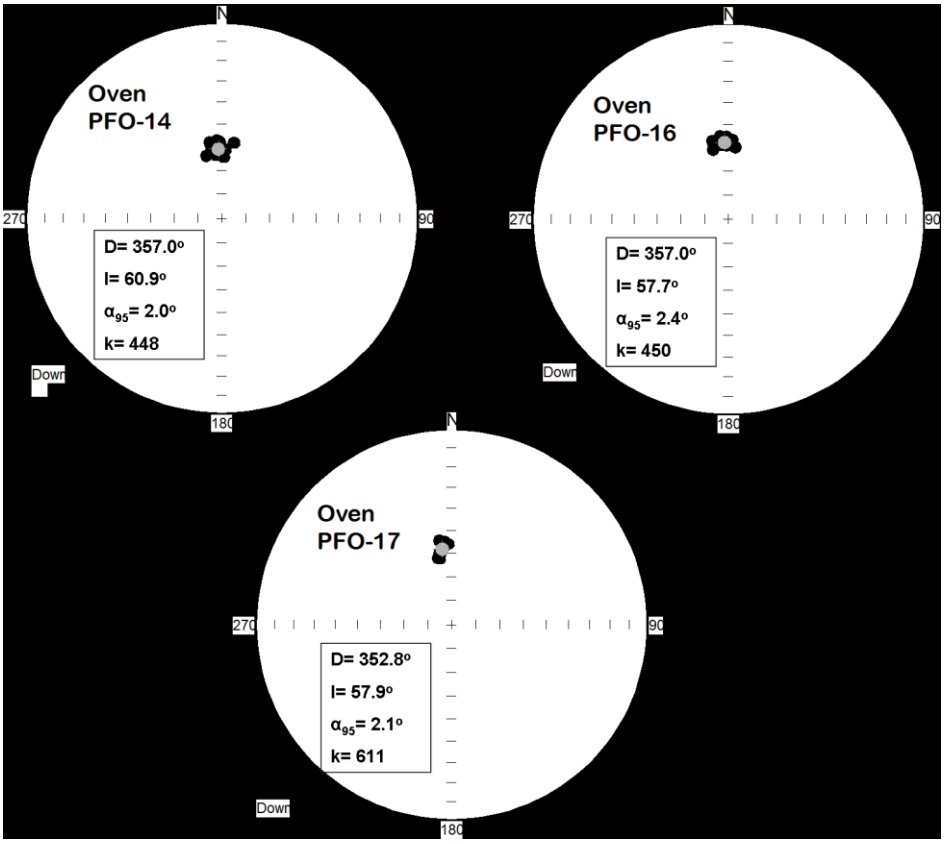
Oven
PFO-14
D= 357.0°
I= 60.9°
α95= 2.0°
k= 448
Oven
PFO-16
D= 357.0°
I= 57.7°
α95= 2.4°
k= 450
Oven
PFO-17
D= 352.8°
I= 57.9°
α95= 2.1°
k= 611
Down

(b)

Fig. 6

826

827

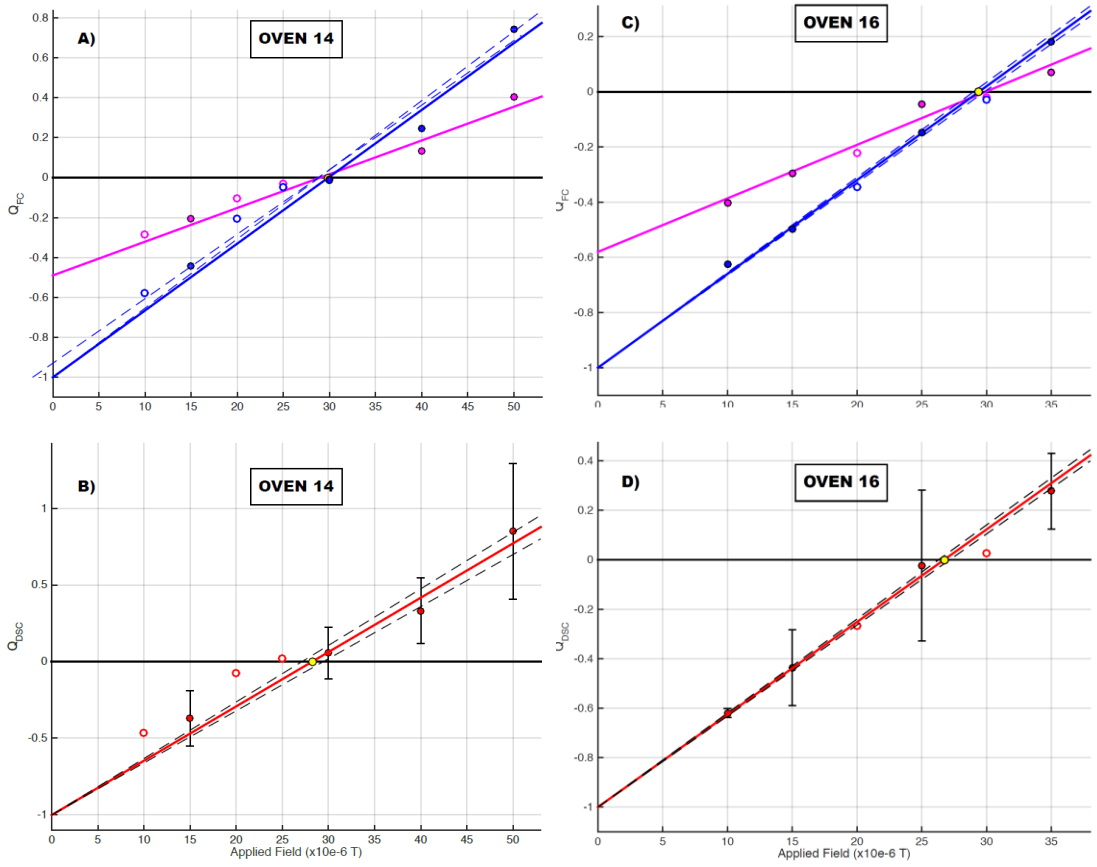

828

829 Fig. 7

830

831

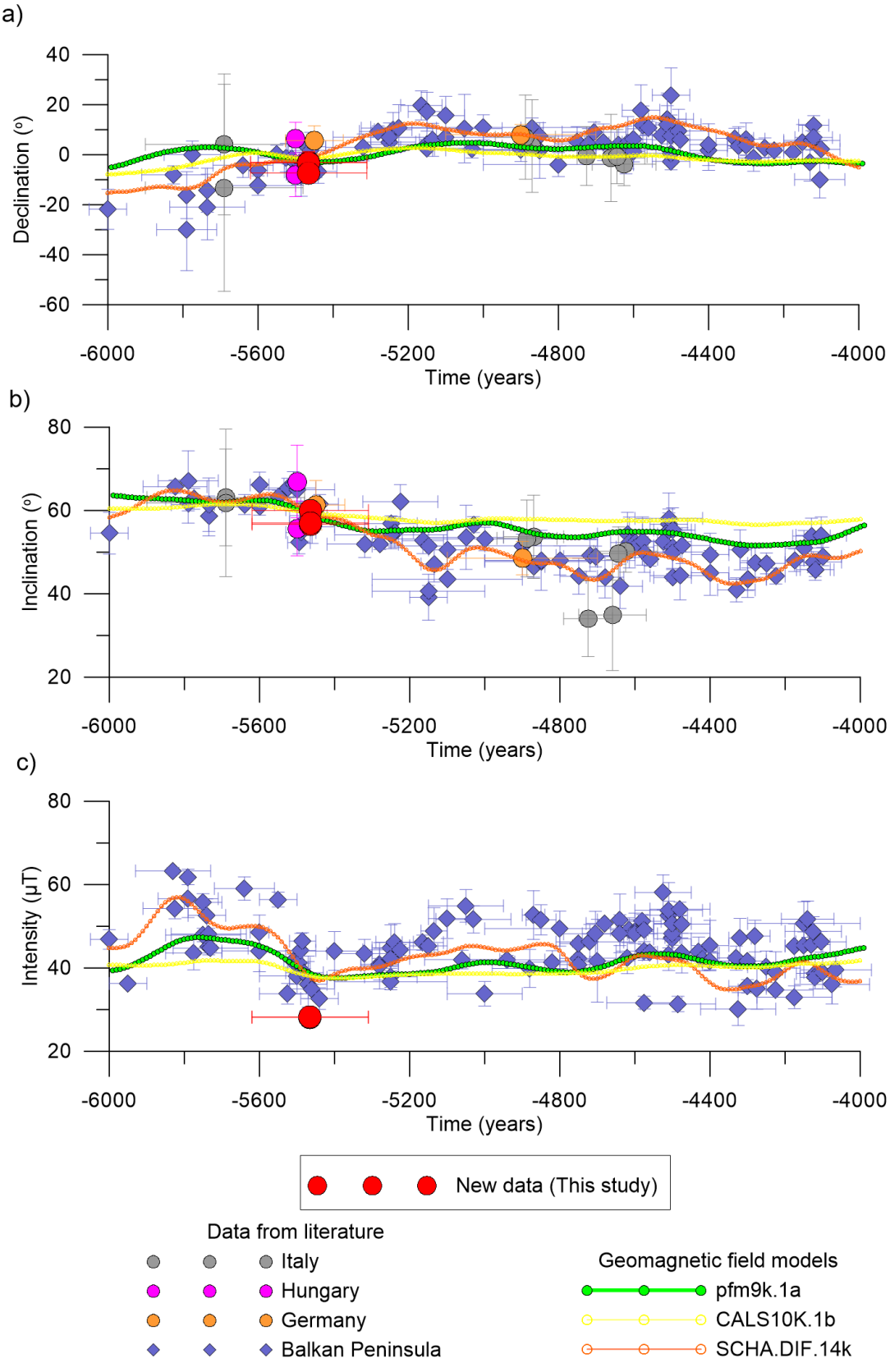
a)
Declination (°)
40
20
0
-20
-40
-60
-6000
-5600
-5200
-4800
-4400
-4000
Time (years)
b)
Inclination (°)
80
60
40
20
-6000
-5600
-5200
-4800
-4400
-4000
Time (years)
c)
Intensity (µT)
80
60
40
20
-6000
-5600
-5200
-4800
-4400
-4000
Time (years)
New data (This study)
Data from literature
Italy
Hungary
Germany
Balkan Peninsula
Geomagnetic field models
pfm9k.1a
CALS10K.1b
SCHA.DIF.14k

Fig. 8

Sample	NRM (E-03 A/m)	Bulk susceptibility (E-03 SI)	P_{AMS}	D (º)	I(º)	MAD
Oven PFO14						
PFO14-1	526.9	4.253	1.011	358.5	57.8	1.3
PFO14-2	233.4	1.681	1.006	351.0	61.4	1.4
PFO14-3	377.0	2.848	1.009	9.3	57.7	0.9
PFO14-4	593.8	4.770	1.002	358.6	61.3	1.4
PFO14-5	351.6	2.548	1.012	354.9	63.4	1.4
PFO14-6	563.3	4.316	1.002	356.1	60.6	1.6
PFO14-7	869.9	5.898	1.011	355.0	61.5	1.3
PFO14-8	456.2	3.973	1.011	346.1	63.0	1.3
PFO14-9	509.8	4.173	1.007	356.4	57.0	2.4
PFO14-12	681.1	4.137	1.008	3.2	61.0	3.5
PFO14-13	705.7	4.648	1.007	2.1	64.3	1.8
PFO14-14	476.3	4.679	1.011	350.9	57.7	1.5
PFO14-15	567.8	4.368	1.006	357.9	63.4	1.6

Mean direction:

N= 13	**D_m= 357.0º**		**I_m= 60.9º**	**α_{95}= 2.0º**	**k=448**	
Oven PFO16						
PFO16-4	1479	7.090	1.007	347.7	60.1	0.7
PFO16-5	1438	6.271	1.007	2.8	56.4	0.9
PFO16-6	751.6	5.539	1.003	5.6	59.5	1.2
PFO16-7	1212	7.036	1.004	354.3	54.8	0.9
PFO16-8	899.2	5.725	1.013	354.8	58.7	1.3
PFO16-9	1022	5.516	1.007	1.7	57.7	1.4
PFO16-11	1399	7.888	1.007	358.9	59.0	1.1
PFO16-12	1223	7.030	1.010	358.8	55.2	1.5
PFO16-13	1110	6.848	1.008	348.4	56.3	1.3
Mean direction:						
N=9	**D_m= 357.0º**		**I_m= 57.7º**	**α_{95}= 2.4º**	**k=450**	
Oven PFO17						
PFO17-7	916.78	9.441	1.003	351.2	59.5	1.9
PFO17-8	1514	10.94	1.002	355.4	55.1	1.4

PFO17-9	2043	12.39	1.023	357.7	56.0	1.0
PFO17-11	2143	10.65	1.004	353.5	57.7	0.9
PFO17-12	1753	10.13	1.002	356.1	56.0	1.3
PFO17-13	2100	13.14	1.004	349.8	61.8	0.9
PFO17-14	2089	14.96	1.003	348.3	61.4	1.4
PFO17-15	1985	11.94	1.005	350.2	59.6	0.9
PFO17-16	2287	12.57	1.003	351.8	54.0	2.5
Mean direction:						
N=9	**D_m= 352.8º**	**I_m= 57.9º**	**α_{95}= 2.1º**	**k=611**		

Table 1

Method	PI (μT)	65% conf.	n/N	R-squared	RMSE
Oven 14					
MSP-DB	29.0	[26.6 - 31.1]	4/7	0.9665	0.0575
MSP-FC	29.9	[28.9 - 30.9]	4/7	0.9766	0.0760
MSP-DSC (α = 0.2)	29.4	[27.1 - 29.4]	4/7	0.9701	0.1845
MSP-DSC (α = 0.8)	27.2	[28.3 - 30.6]	4/7	0.9546	0.1866
MSP-DSC (α = 0.5)	**28.2**	**[27.1 - 29.4]**	**4/7**	**0.9630**	**0.1842**
Oven 16					
MSP-DB	29.9	[28.3 - 31.9]	4/7	0.9746	0.0425
MSP-FC	29.4	[29.0 - 29.8]	4/7	0.9968	0.0205
MSP-DSC (α = 0.2)	27.8	[27.2 - 28.4]	4/7	0.9942	0.1076
MSP-DSC (α = 0.8)	25.7	[25.2 - 26.2]	4/7	0.9957	0.0860
MSP-DSC (α = 0.5)	**26.7**	**[26.3 - 27.2]**	**4/7**	**0.9972**	**0.0711**
Oven 17					
MSP	n.d.	n.d	3/7	n.d	n.d

Table 2